
Research Article: New Research | Cognition and Behavior

Theta-gamma cross-frequency transcranial alternating current stimulation over the trough impairs cognitive control

<https://doi.org/10.1523/ENEURO.0126-20.2020>

Cite as: eNeuro 2020; 10.1523/ENEURO.0126-20.2020

Received: 2 April 2020

Revised: 15 July 2020

Accepted: 15 July 2020

This Early Release article has been peer-reviewed and accepted, but has not been through the composition and copyediting processes. The final version may differ slightly in style or formatting and will contain links to any extended data.

Alerts: Sign up at www.eneuro.org/alerts to receive customized email alerts when the fully formatted version of this article is published.

Copyright © 2020 Turi et al.

This is an open-access article distributed under the terms of the Creative Commons Attribution 4.0 International license, which permits unrestricted use, distribution and reproduction in any medium provided that the original work is properly attributed.

1 1. **Manuscript title:** Theta-gamma cross-frequency transcranial alternating current stimulation
2 over the trough impairs cognitive control

3 2. **Abbreviated title (50 character max):** Theta-gamma tACS alters cognitive control

4 3. **List of authors and affiliations:** Zsolt Turi^{1,2*}, Matthias Mittner^{3*}, Albert Lehr¹, Hannah
5 Bürger¹, Andrea Antal¹, and Walter Paulus¹

6 *Equal contribution

7 ¹Department of Clinical Neurophysiology, University Medical Center Göttingen, Göttingen 37073,
8 Germany

9 ²Department of Neuroanatomy, Institute of Anatomy and Cell Biology, Faculty of Medicine,
10 University of Freiburg, Freiburg, Germany.

11 ³Department of Psychology, UiT The Arctic University of Norway

12 4. **Author contributions**

13 ZT: conceptualization, study design, project administration, methodology, software (behavioral
14 paradigm), supervised data collection, supervised medical student, prepared illustrations, data
15 visualization, interpreted data, data curation, wrote original draft and revised manuscript.

16 MM: formal statistical analysis, data visualization, computational modelling of behavioral data,
17 interpreted data, data curation, wrote original draft and revised manuscript.

18 AL: contributed to formal analysis, contributed to preparing illustrations, data visualization,
19 interpreted data and wrote original draft and revised manuscript.

20 HB: data collection (as part of her medical dissertation at the University Medical Center
21 Göttingen, Germany, supervised by author AA), transcribed data, contributed to writing original
22 draft and revised manuscript.

23 AA: project administration, supervised medical student, contributed to writing original draft and
24 revised manuscript.

25 WP: study design, resources and funding acquisition, contributed to writing original draft and
26 revised manuscript.

27 5. **Correspondence** should be addressed to Zsolt Turi (zsoltturi@gmail.com) and Matthias
28 Mittner (matthias.mittner@uit.no)

29 6. Number of **Figures** : 5

30 7. Number of **Tables**: 1

31 8. Number of **Multimedia**: 1

32 9. Number of words for **Abstract**: 247

33 10. Number of words for **Significance Statement**: 76

34 11. Number for words for **Introduction**: 750

35 12. Number of words for **Discussion**: 1580

36 13. **Acknowledgements**: The authors wish to thank Dr. med. Anja Manig, Dr. med. Sebastian
37 Schade, Dr. med. Dirk Czesnik and Dr. med. Claire Halsband for the neurological examinations.
38 We thank Prof. Thomas Crozier for his comments on the manuscript.

39 14. **Conflict of interest**: Authors report no conflict of interest.

40 15. **Funding sources**: This research was financially supported by DFG PA 419/15-1 awarded to
41 WP. AL was supported by the IMPRS Neurosciences. AA was supported by the State of Lower
42 Saxony, Germany (76251-12-7/19 (ZN 3456))

43 16. **Link to repository**: https://github.com/ihrke/2020_cfc_tacs

44

45 Theta-gamma cross-frequency transcranial alternating current
46 stimulation over the trough impairs cognitive control

47

48 Zsolt Turi^{1,2*}, Matthias Mittner^{3*}, Albert Lehr¹, Hannah Bürger¹, Andrea Antal¹, and
49 Walter Paulus¹

50 *Equal contribution

51 ¹Department of Clinical Neurophysiology, University Medical Center Göttingen,
52 Göttingen 37073, Germany

53 ²Department of Neuroanatomy, Institute of Anatomy and Cell Biology, Faculty of
54 Medicine, University of Freiburg, Freiburg, Germany.

55 ³Department of Psychology, UiT The Arctic University of Norway

56

57 **Correspondence** should be addressed to Zsolt Turi (zsoltturi@gmail.com) and Matthias
58 Mittner (matthias.mittner@uit.no)

59 **Abstract**

60 Cognitive control is a mental process, which underlies adaptive goal-directed decisions.
61 Previous studies have linked cognitive control to electrophysiological fluctuations in the
62 theta band and theta-gamma cross-frequency coupling (CFC) arising from the cingulate
63 and frontal cortices. Yet, to date the behavioral consequences of different forms of theta-
64 gamma CFC remain elusive. Here, we studied the behavioral effects of the theta-gamma
65 CFC via transcranial alternating current stimulation (tACS) designed to stimulate the
66 frontal and cingulate cortices in humans. Using a double-blind, randomized, repeated
67 measures study design, 24 healthy participants were subjected to three active and one
68 control CFC-tACS conditions. In the active conditions, 80 Hz gamma tACS was coupled
69 to 4 Hz theta tACS. Specifically, in two of the active conditions, short gamma bursts
70 were coupled to the delivered theta cycle to coincide with either its peaks or troughs. In
71 the third active condition, the phase of a theta cycle modulated the amplitude of the
72 gamma oscillation. In the fourth, control protocol, 80 Hz tACS was continuously
73 superimposed over the 4 Hz tACS, therefore lacking any phase-specificity in the CFC.
74 During the 20-minute of stimulation, the participants performed a Go/NoGo monetary
75 reward- and punishment-based instrumental learning task. A Bayesian hierarchical
76 logistic regression analysis revealed that relative to the control, the peak-coupled tACS
77 had no effects on the behavioral performance, whereas the trough-coupled tACS and, to
78 a lesser extent, amplitude-modulated tACS reduced performance in conflicting trials. Our
79 results suggest that cognitive control depends on the phase-specificity of the theta-
80 gamma CFC.

81 **Statement of significance**

82 This study investigated the behavioral effects of different forms of theta-gamma cross-
83 frequency coupling in cognitive control. To this aim, we delivered cross-frequency
84 transcranial alternating current stimulation over the cingulate and frontal cortices in
85 humans. We found that when gamma tACS was coupled to the trough of theta tACS, the
86 stimulation worsened the ability of healthy participants to employ cognitive control. Our
87 findings highlight the role of theta-gamma cross frequency coupling in complex goal-
88 directed behavior in humans.

89 **1. Introduction**

90 In goal-directed behavior, contextual and reward-related information should be
91 effectively linked to form action plans in order to accomplish goals and perform decisions
92 in a flexible and prospective manner (Helfrich & Knight, 2019). In humans, at least three
93 main behavioral control systems influence the decisions: The Pavlovian system, the
94 model-free and the model-based instrumental systems (Guitart-Masip et al., 2014). The
95 Pavlovian system is responsible for automatic, reflexive response tendencies that
96 depend on the valence of the stimulus. It facilitates approaching behavior for rewarding
97 stimuli and response inhibition for unrewarding ones (Guitart-Masip et al., 2014). The
98 model-free system gradually incorporates the behavioral consequences of actions by
99 computing the difference between the predicted and received outcome. The model-
100 based system creates an internal world model, which enables flexible, prospective
101 planning. Therefore, decisions do not exclusively rely on the outcome history (Helfrich &
102 Knight, 2019).

103 Conflict can arise between the Pavlovian and instrumental behavioral control
104 systems, when the evolutionary hard-wired, valence-response associations do not
105 support adaptive behavior. This situation occurs when approaching rewards is
106 maladaptive, or when rewards can be secured by response inhibition rather than by
107 approach (Guitart-Masip et al., 2012). Cognitive control is a mental process for resolving
108 this conflict between the behavioral control systems (Guitart-Masip et al., 2014; Shenhav
109 et al., 2017).

110 The oscillatory activity in the theta and gamma frequency bands and their interaction
111 may play a crucial role in cognitive control (Cavanagh & Frank, 2014; Cohen, 2014).
112 Theta-gamma, phase-amplitude cross-frequency coupling (CFC) is one form of such

113 interaction, where the phase of the theta oscillation modulates the amplitude of the
114 gamma oscillation (Canolty & Knight, 2010). Human intracranial electrophysiological
115 recordings revealed that theta-gamma, phase-amplitude CFC in the anterior cingulate
116 cortex (ACC) and dorsolateral prefrontal cortex (DLPFC) emerges during cognitive
117 control (Smith et al., 2015). E.g., Smith and colleagues found that the amplitude of the
118 high gamma oscillation was highest in a specific phase range of the theta oscillation (ca.
119 0° - 60°) during a cognitive control task (Smith et al., 2015).

120 To study how participants learn to overcome the Pavlovian bias by utilizing cognitive
121 control mechanisms, we used a probabilistic Go/NoGo instrumental learning task
122 (Cavanagh et al., 2013). We tested the behavioral relevance of theta-gamma cross-
123 frequency coupling in humans via transcranial alternating current stimulation (tACS),
124 which can externally generate oscillating electric fields in the brain (Peterchev et al.,
125 2012). We utilized three CFC-tACS protocols delivered in the theta and gamma
126 frequency bands: Peak- and trough-coupled tACS and amplitude-modulated tACS
127 (Alekseichuk et al., 2016; Amador de Lara et al., 2017; Minami & Amano, 2017). In the
128 context of the present study, the notion of peak and trough refers to the local maximum
129 and minimum of the amplitude of the delivered theta tACS wave, to which the short
130 gamma tACS burst was coupled. In the amplitude-modulated protocol, the amplitude of
131 the gamma oscillation was modulated by the phase of the theta wave.

132 We hypothesized that the peak-coupled tACS would improve the accuracy and/or the
133 speed of learning relative to the control stimulation. We based this hypothesis on the
134 notion that these protocols mimic the phase-specificity of theta-gamma CFC when
135 signaling the need for cognitive control (Smith et al., 2015). Moreover, we also
136 anticipated that the trough-coupled tACS would impair behavioral performance because

137 this pattern is contrary to that activity naturally occurring during the successful
138 implementation of cognitive control (Smith et al., 2015). Third, we expected that
139 modulating the CFC between the ACC and DLPFC via CFC-tACS protocols should
140 affect the amount of Pavlovian bias. In particular, facilitating the CFC between the ACC
141 and DLPFC via the peak-coupled tACS would be thought to increase the efficacy of the
142 ACC to signal the need for cognitive control and thereby increase the degree of model-
143 based control implemented by the DLPFC (Smith et al., 2015). This, in turn, might lead
144 to a decreased amount of Pavlovian bias. On the other hand, disrupting the CFC
145 between the ACC and the DLPFC via the trough-coupled tACS should decrease the
146 efficacy of signaling the need for cognitive control. This may impair the efficacy of
147 implementing model-based control and therefore lead to a higher degree of Pavlovian
148 bias. Fourth, we expected that amplitude-modulated tACS would improve behavioral
149 performance by entraining the ongoing theta oscillation by the envelope of the high
150 frequency stimulation (Negahbani et al., 2018). The amplitude-modulated tACS protocol
151 would increase the theta synchrony in the cingulate and frontal cortices (Negahbani et
152 al., 2018), which in turn would improve the ability of the participants to apply cognitive
153 control.

154

155 **2. Methods**

156 **2.1. Participants**

157 Twenty-four healthy, native German-speaking adult volunteers (12 female, mean age
158 \pm SD: 23.0 ± 3.26 years, age range from 18 to 30 years) joined the study. This number
159 of participants was chosen to allow a complete randomization of the order of the four
160 tACS protocols (*i.e.*, three active and one control protocols), and is calculated as four

161 factorial or 24. The mean number of years of education (\pm SD) was 16.30 ± 3.05 (range
162 from 12 to 22.5 years). Before entering the study, the participants were informed about
163 possible adverse effects of tACS, and all of them gave their written informed consent.
164 The exclusion criteria were history or presence of current medical, neurological or
165 psychiatric illnesses including epilepsy, drug and/or alcohol addiction and the presence
166 of metal implants in the head, neck and chest. In addition, the participants were
167 examined by neurologists at the Department of Clinical Neurophysiology, University
168 Medical Center Göttingen. The study neurologist evaluated whether any of the exclusion
169 criteria were met. None of the participants reported any neurological or psychiatric
170 disorders, drug-dependency, or medication acting on the central nervous system prior to
171 or during the experiment.

172

173 **2.2. Code accessibility, data availability and ethic statement**

174 The Ethics Committee of the University Medical Center Göttingen approved the
175 study, the study protocols, and all methods used therein. We performed the study in
176 accordance with relevant guidelines and regulations. The study was registered under the
177 study approval number 20/5/15. The study materials, code/software and pseudonymized
178 raw data described in the paper is freely available online at
179 https://github.com/ihrke/2020_cfc_tacs.

180

181 **2.3. Experimental design**

182 The study used a double-blind, within-subject design. The participants underwent five
183 experimental sessions, starting with an initial training session to familiarize themselves
184 with the behavioral paradigm. During the training session, the participants received no

185 stimulation. This initial session was followed by the four tACS sessions, the order of
186 which was counterbalanced across participants to reduce between-session learning
187 effects. Of the four stimulation sessions, three employed the main stimulation protocols
188 and one the control protocol. The inter-session interval between the stimulation sessions
189 was at least 48 hours.

190

191 **2.4. Behavioral Paradigm**

192 The behavioral paradigm consisted of a learning phase and a subsequent transfer
193 phase, which was adapted from Cavanagh and colleagues (2013). The task was
194 introduced as a card game for the participants (Figure 1). Stimuli presentation was
195 controlled by PsychoPy (version number: 1.83.01), a free, open-source application built
196 on the Python programming language (Peirce, 2007, 2009). For the presentation of the
197 behavioral paradigm, we used a Dell computer with Windows 7 Enterprise 64 bit
198 operating system, Intel (R) core i3-3220, 3.30 GHz and 4 GB RAM and a 21.5 inch Dell
199 screen with a 1920 × 1080 resolution and 60 Hz refresh rate.

200 During the learning phase the participants performed a Go/NoGo instrumental
201 learning task. Here, they had to learn action (two levels: Go/NoGo) and monetary
202 outcome (three levels: win, no win/lose or lose) contingencies. For each card, the goal
203 was to find the better of the two possible action choices (Go/NoGo) resulting in the
204 highest monetary outcome (getting reward or avoiding losing) and therefore maximize
205 their earnings.

206 One key feature of the task was that the action choices and monetary outcomes
207 were orthogonal. As such, the four unique cards covered all the combinations between
208 actions choices and monetary outcomes ('Go to win', 'NoGo to avoid losing', 'Go to avoid

209 losing' and 'NoGo to win'). Due to the Pavlovian bias, *i.e.*, approach to appetitive and
210 withdrawal from aversive stimuli, the cards could be split into congruent and conflicting
211 cards. For the Pavlovian congruent cards (henceforth the congruent cards; 'Go to win'
212 and 'NoGo to avoid losing') the action selection under the automatic, Pavlovian bias was
213 advantageous for the participants and hence easier to learn. For the Pavlovian
214 conflicting cards (henceforth the conflicting cards; 'NoGo to win' and 'Go to avoid
215 losing'), the action selection under the automatic, Pavlovian bias was disadvantageous
216 for the participants and therefore harder to learn (Guitart-Masip et al., 2012).

217 The action outcomes were probabilistic such that 65% of correct responses led to a
218 better outcome: Neutral monetary outcomes (no loss) for the lose cards and monetary
219 reward for the win cards. Consequently, 35% of the correct responses led to neutral
220 monetary outcomes for the win cards and monetary loss for the lose cards. On the other
221 hand, wrong responses inverted this ratio, *i.e.* 65 % of incorrect responses led to neutral
222 monetary outcomes for the win cards and monetary loss for the lose cards. Previous
223 studies used 80% vs. 20% or 70% vs. 30% action-outcome contingencies, which
224 renders the present version of the probabilistic learning task slightly more difficult
225 compared with previous versions (Cavanagh et al., 2013; Csifcsák et al., 2020; Guitart-
226 Masip et al., 2012).

227 For illustrative purposes, we describe possible action-outcome scenarios. Suppose
228 card A was a 'Go to Win' card, a fact unknown to the participant. In case the participant
229 decided to take the card, there was a 0.65 probability to receive the feedback indicating
230 monetary reward. Consequently, there was a 0.35 probability to receive no reward. In
231 case the participant did not take the 'Go to Win' card, the feedback probabilities were

232 reversed. That is, the probability of receiving monetary reward was 0.35 and the
233 probability of receiving no reward was 0.65.

234 Each card was presented 20 times in a random order. Independent sets of five cards
235 were used and randomly chosen for each session from a pool of six sets of cards. We
236 created six card sets for the scenario that one session has to be repeated. Therefore,
237 participants performed 80 trials in each session (20 trials × four cards) and 400 trials in
238 total (80 trials × five sessions).

239 The presentation of the stimuli was performed in full screen mode. We set the
240 background color of the screen to white. At the beginning of each trial, a black fixation
241 cross (10 or 11 s) was presented (see Figure 1A, Trial flow). Note that we used a
242 relatively long duration of fixation cross in the present study compared with previous
243 studies (e.g., Guitart-Masip et al., 2012). Also, during this time the participants were
244 instructed to blink and swallow. This was a necessary step to increase the comparability
245 of the present results with our other experiments using pre-stimulus intermittent tACS
246 (manuscript in preparation) and scalp electroencephalogram recordings.

247 Then a card cue (1 s; original image size 199 × 279 pixels, presentation size 0.3 ×
248 0.5) was presented to the participants. We used white cards and distinguished them with
249 a black capital letter (B, C, D, F, G, H, J, K, R, S, T, V, A, E, O, U, L, M, P, Q, W, X, Y, Z)
250 printed in the middle of the card (see Figure 1A, Trial flow). We decorated the cards by
251 adding four pieces of simple shapes around the letter. We used rhombus, circle and
252 rectangle shapes and filled them with blue, gray, green, pink, orange or yellow colors. In
253 each set, we used the same shape and color for each card.

254 The target detection stimulus (black circle; original image size 225 × 220 pixels,
255 presentation size 0.35 × 0.45) was shown until a response occurred, or 1 s passed. The

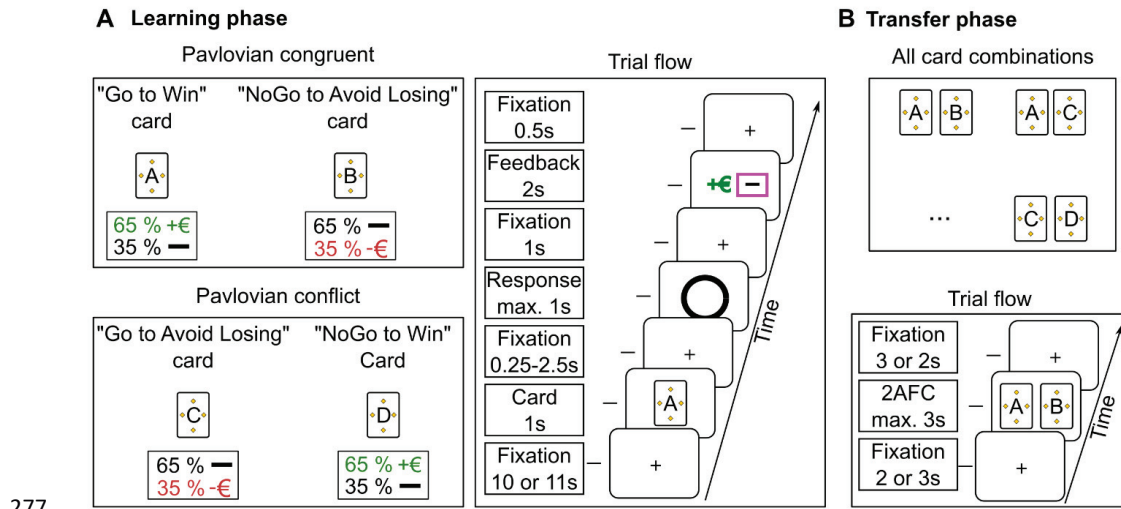
256 target detection stimulus indicated to the participants that they could take the card (Go)
257 or not (NoGo), upon which the monetary outcome depended. The feedback was
258 displayed (original image size 402 × 205 pixels, presentation size 0.6 × 0.4) for 2 s: A
259 green '+€' sign indicated a monetary reward, a red '-€' symbol indicated a monetary loss
260 and a black horizontal bar indicated neutral monetary outcome (neither win nor loss).
261 The next trial started 0.5 s after feedback.

262 In the subsequent transfer phase of the task (Figure 1B), the participants performed
263 a two-alternative, forced-choice (2AFC) task where each card from the learning phase
264 was paired with one of the three other cards following the order (e.g., 'Go to win' vs.
265 'NoGo to avoid losing', 'NoGo to avoid losing' vs. 'Go to win', etc.). Each of the 12 card
266 pairs was presented four times until a response occurred, or 3 s passed.

267 The dependent variable in this study was accuracy. We defined accuracy as
268 choosing the response category (Go/NoGo) that led with a higher probability to the
269 better monetary outcome; hence, monetary reward for the win cards and neutral
270 monetary outcome for the losing cards.

271 The participants were paid 8 EUR/hour and received an additional performance
272 dependent bonus of 12 EUR if their mean performance calculated over all sessions was
273 above 75 %. We used the monetary bonus to encourage our participants to perform as
274 well as possible in each session. Unknown to the participants, everybody received the
275 monetary bonus at the end of the experiment.

276



277

278 **Figure 1.** The structure and the trial flow of the behavioral paradigm for the learning (A)
 279 and the transfer phase (B).

280

281 **2.5. Transcranial alternating current stimulation**

282 The stimulation was delivered by a CE-certified NeuroConn® multichannel stimulator
 283 (neuroConn GmbH, Ilmenau, Germany) during the learning phase of the task. The
 284 electrode positions were chosen according to the international 10-20 EEG system. The
 285 electrode montage was centered over the Fpz electrode location with three return
 286 electrodes positioned over the Cz, F10 and F9 positions (Figure 2A).

287 The following standardized steps ensured minimal stimulation-induced cutaneous
 288 sensations. After determining the electrode locations, the corresponding skin surface
 289 was gently cleaned with OneStep® abrasive gel (H + H Medizinprodukte GbR,
 290 Germany), which was removed with 0.9 % saline solution (B. Braun Melsungen AG,
 291 Germany). After removing the residual saline solution with paper tissue a local
 292 anesthetic cream (Anesderm®, Pierre Fabre Dermo-Kosmetic GmbH, Germany) was

293 applied for 20 min to numb the skin (25 mg/g lidocaine, 25 mg/g prilocaine). It was wiped
294 off first with paper tissue followed by a skin antiseptic spray (Kodan Tinktur Forte®,
295 Schuelke & Mayr GmbH, Germany). The latter was necessary to remove the anesthetic
296 cream, which would otherwise prevent the conductive paste from adhering to the skin.
297 Homogenous layers of Ten20® conductive paste (Waever and Company, Colorado,
298 USA) were then applied to the skin and the electrode surfaces. Each of the four round,
299 conductive rubber electrodes with 2 cm diameter (neuroConn GmbH, Germany) was
300 affixed to the head. The impedance was kept below 10 kΩ. The maximal current density
301 under the main electrode was 0.50 mA/cm². The electrode montage was prepared in a
302 double-blind fashion.

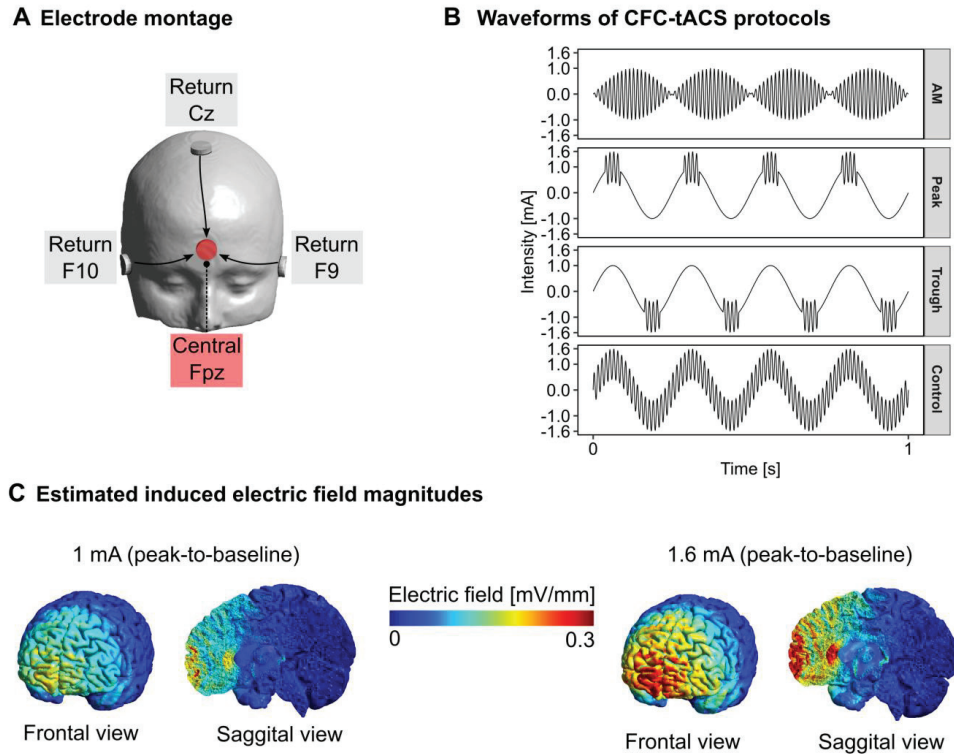
303 We used four different CFC-tACS protocols, including amplitude-modulated CFC-
304 tACS (AM), CFC over the peak, trough and control tACS (Figure 2B). Each protocol
305 started with a 20s fade-in period, followed by a 20-min stimulation with the maximum
306 stimulation intensity, and ended with a 10s fade-out period. The total stimulation duration
307 was 20 min and 30 s.

308 The protocols, peak-coupled, trough-coupled tACS and control, consisted of a 4 Hz,
309 1 mA (=2 mA peak to peak) sinusoidal waveform coupled with a 0.6 mA (=1.2 mA peak
310 to peak) 80 Hz sinusoidal waveform. These stimulation protocols had a maximum
311 intensity of 1.6 mA. In the peak-coupled tACS protocol, the short 80 Hz burst (50 ms)
312 was coupled over the peak (38-88 ms) of each theta cycle. In the trough-coupled tACS
313 protocol, the short 80 Hz burst was coupled over the trough (163-213 ms) of each theta
314 tACS cycle. In the control stimulation, both waveforms were overlaid continuously. The
315 control stimulation lacked any phase-specificity of gamma relative to theta oscillations
316 but used a highly matched intensity range and identical stimulation duration with respect

317 to the real protocols. The control protocol served as the reference to which we compared
318 the effects of the three main CFC-tACS protocols.

319 In the AM protocol, the amplitude of the gamma frequency (80 Hz) was modulated by
320 the phase of the theta frequency (4 Hz). In all protocols, the amplitude of the theta
321 frequency was constant. Consequently, the AM protocol employed lower peak
322 stimulation intensities (Figure 2C, left) compared with the remaining protocols, which led
323 to a slightly higher electric field strength (Figure 2C, right). However, this was a
324 necessary step in order to match the amplitude of the envelope frequency in the
325 amplitude modulation protocol to the amplitude of the theta frequency in the remaining
326 protocols.

327 In order to estimate the magnitude of the induced electric field in the brain, we ran
328 simulations using the free software package Simulations for Non-invasive Brain
329 Stimulation (SimNIBS; version 3.0.2) (Thielscher et al., 2015). To this aim, we conducted
330 electric field calculations on an anatomically realistic, six-compartment template head
331 model (almi5.msh) available in SimNIBS. We used default conductivity values [S/m] that
332 were set to 0.465 for the scalp, 0.01 for skull, 1.654 for cerebrospinal fluid, 0.275 for
333 gray matter and 0.126 for the white matter. The simulation accounted for volume-
334 normalized anisotropy in the brain. We observed peak electric field magnitudes up to 0.3
335 mV/mm in the medial frontal cortex (Figure 2C, right).



336

337 **Figure 2.** Stimulation parameters including electrode montage (A), cross-frequency-
 338 coupling tACS waveforms (B) and estimated electric field magnitudes in the gray matter.
 339 Electric field simulations were performed with SimNIBS version 3.0.2 on a template head
 340 model. The peak absolute electric field strength reached 0.3 mV/mm in the medial frontal
 341 cortex. Abbreviations: AM – amplitude-modulated; CFC – cross-frequency coupling.

342

343 2.6. Procedure

344 At the start of each session, the participants filled out a short questionnaire. We
 345 asked our participants to report the quality of sleep during the previous night. Further,
 346 we assessed the level of arousal (“*How are you feeling right now?*”) with a 10-point
 347 Likert-scale where value 1 corresponded to very tired and 10 to completely awake. We

348 also assessed the presence and intensity of headache (“*Do you have a headache right*
349 *now?*”) with an initial yes-no answer and an optional 10-point Likert-scale for yes
350 responses. Here, value 1 corresponded to low and 10 to very strong headache. We
351 assessed the intake of medication, coffee or alcohol consumption in the 24 hours before
352 the session. The purpose of these assessments was to avoid the possibility that irregular
353 sleep patterns in the previous night, headache or mental fatigue due to alcohol would
354 corrupt the possible behavioral findings of tACS. Theoretically, a new session was going
355 to be scheduled if the participant had consumed more than two alcoholic beverages in
356 the previous day, however, arranging a new session was not necessary.

357 All participants received detailed written instructions about the task. Before the
358 training session, we asked them to perform a practice session to familiarize themselves
359 with the task and to ensure that they were able to operate the response box (RB-740,
360 Cedrus Corporation, USA) comfortably. We used an independent set of cards in the
361 practice session. Before the start of the learning task, the participants filled out a
362 questionnaire to ensure that they understood the tasks correctly. The questionnaire
363 assessed whether the participants understood i) the meaning of the three feedback
364 types (win, no win/no loss, loss) and ii) the probabilistic nature of the feedback.

365 In the following stimulation sessions, the short questionnaire was followed by the
366 electrode preparation, the application of the topical anesthetic cream, and the
367 impedance measurements. This preparation phase took approx. 35-40 minutes during
368 which the participants watched documentary movies to maintain their vigilance.

369 Following the preparatory phase, the participants performed two short practice
370 tasks. The practice tasks contained 16 trials for the learning and 12 trials for the transfer
371 phase.

372 Following the practice task and directly before the start of the learning task, the
373 data collector opened the sealed envelope containing the information about that day's
374 stimulation condition. After opening the envelope, the data collector selected the
375 protocol on the stimulator and informed the participants about the start of the stimulation.

376 Following this moment, the data collector initiated no further communication. The
377 learning phase began directly after the fade-in period. After the end of learning phase
378 and following a 5-minute break, the participants completed the transfer phase of the
379 task, during which no stimulation was applied.

380 At the end of each session, we assessed the level of self-reported arousal, the
381 presence and intensity of headache and secondary perceptual adverse effects
382 associated with the application of tACS. We focused on cutaneous (*i.e.*, itching, tingling
383 and burning) and visual flickering sensations (*i.e.*, phosphenes). First, the participants
384 were asked to indicate the presence of secondary adverse effects (yes or no question).
385 In case of a positive answer, we assessed the subjective level of discomfort using a 10-
386 point Likert scale. On the Likert scale, "1" indicated the lowest noticeable discomfort and
387 "10" indicated an amount of discomfort the participants would not be able to endure
388 during the experiment. The participants were informed that they could discontinue the
389 study at any time without having to give any reason for terminating the study.

390 At the end of each session, we asked our participants to recall the card types and
391 provide an internal ranking of the cards. We focused on whether the participants were
392 able to correctly recall the cards' valence-action contingency.

393

394 **2.7. Statistical analysis**

395 All statistical analyses were performed using the R statistical programming
396 environment (version 3.5.1) and the RStudio integrated development environment
397 (version 1.1.456) (R Core Team, 2018; R Studio Team, 2016). For the data analysis, we
398 used a Precision 7920 Rack computer, Debian GNU/Linux 9.9 operating system, 2 ×
399 Intel Gold 6152, 2.1GHz, 22 cores and 512 GB RAM.

400 We applied Bayesian methods, and we report our results in terms of the mean of the
401 posterior distribution and their associated 95% highest-density intervals (HDIs). These
402 intervals are derived from the posterior distribution of the model-parameters or a
403 combination of parameters (e.g., differences) by finding the interval that contains 95% of
404 the posterior mass while also satisfying the criterion that all points within the interval
405 have a higher probability density than points outside the interval (Kruschke, 2014). The
406 interpretation of the Bayesian 95% HDI is that it gives the range in which the estimated
407 parameter is located with a probability of 0.95. We consider effects to be statistically
408 reliable, if the 95% HDI excludes zero.

409 In order to model accuracy on the single-trial level, a dichotomous dependent
410 variable, we used hierarchical Bayesian logistic regression. For these regression
411 analyses, we used the R package *brms* (Bayesian Regression Models using Stan;
412 Bürkner, 2018) with default, uniform priors for all regression coefficients. This package
413 uses Hamiltonian Monte-Carlo (HMC) techniques implemented in Stan (Carpenter et al.,
414 2017) to fit the models. We used four chains, where each chain had a warm-up period of
415 1,000 samples and 1,000 post warm-up samples resulting in a total of 4,000 posterior
416 samples. We used the Gelman-Rubin diagnostic (Gelman & Rubin, 1992) to ensure that
417 all reported results had an $\hat{R} \leq 1.05$. For model comparison, we used the Leave-One-

418 Out Information Criterion (LOOIC), where lower scores of the LOOIC suggest a better
419 model fit (Vehtari et al., 2017). Specifically, a model was considered better if the LOOIC
420 score were lower, and if the Δ LOOIC score were at least double the corresponding
421 LOOIC standard error.

422

423 **2.8. Computational modelling**

424 The orthogonal Go-NoGo task used in our study usually allows one to fit
425 computational reinforcement learning (RL) models to the data collected during the
426 experiment (e.g., Cavanagh & Frank, 2014; Csifcsák et al., 2020). These models
427 assume that each time a certain stimulus is encountered, an internal value
428 representation of the stimulus-action pair (known as Q-value) is updated according to
429 the reward received after taking an (in-) action. Furthermore, the decision on which
430 action to take is based on this internal value-representation, and thus, as the Q-value
431 gets close to the actual value with repeated encounters of a stimulus, performance
432 becomes more accurate. The orthogonalized nature of the Go-NoGo task typically also
433 allows the estimation of Pavlovian influences on this RL process by biasing Go-
434 responses for rewarding stimuli and NoGo-responses for punished stimuli. We used
435 Bayesian hierarchical modeling to fit a series of these models to our data using a
436 strategy identical to that presented in Csifcsák and colleagues (2020), and we refer the
437 reader to this paper and the data-repository for this paper at
438 https://github.com/ihrke/2020_cfc_tacs for technical details of the RL model. The model-
439 code was based on a the hBayesDM toolbox (Ahn et al., 2017).

440 The described computational models were implemented using the R-package rstan
441 (Stan Development Team, 2018). We used eight parallel chains with a total of 8,000

442 post-warm up samples from the posterior distribution. The convergence diagnostics
443 were identical with the other models as described above.

444

445 **3. Results**

446 **3.1. Computational modeling**

447 We fitted models of increasing complexity to the data from our experiment. First, we
448 fitted a model without any session-specific terms (null-model) as a baseline. Next, we
449 modeled separate learning-rates α , temperature parameters β , Pavlovian bias
450 parameters π and go-biases b for each of the tACS sessions (tACS-model).
451 Furthermore, we included a model that let each of the four core-parameters depend on
452 the session order (order-model) and, finally, a model where separate parameters were fit
453 for each tACS session and each parameter depended on session-order (full model).
454 Diagnostics of the HMC chains indicated that all models converged successfully.

455 We calculated the LOOIC for each of these models (see Table 1). Even though the
456 model that only modeled the RL parameters as a function of session order received the
457 lowest LOOIC, the differences between all four models were small compared to their
458 standard errors (see Table 1) and model selection was therefore inconclusive. We
459 conducted posterior predictive checks and simulated 1,000 random datasets from the
460 posterior distribution of the parameters. Unfortunately, while some general
461 characteristics of our participants' performance was captured by the model, it failed to
462 properly account for the complex changes across sessions, trials and card types. Given
463 that the computational models were unable to capture our participants' behavior, we
464 chose not to interpret or report changes in model parameters across sessions but to
465 focus on the more descriptive logistic regression models reported below. The reason for

466 our failure to model our participants' performance with these established models is
467 puzzling and deserves further investigation.

468

469 **Table 1.** Results of the model selection procedure for the computational models. All
470 differences in LOOIC are small compared to their standard errors and model selection is
471 therefore inconclusive.

472

Model	LOOIC	Δ LOOIC	SE(Δ LOOIC)
Order	10598.3	–	–
Full	10607.8	9.6	30.2
tACS	10608.5	10.2	39.4
Null	10615.3	17.0	33.2

473

474

475 **3.2. Accuracy and learning**

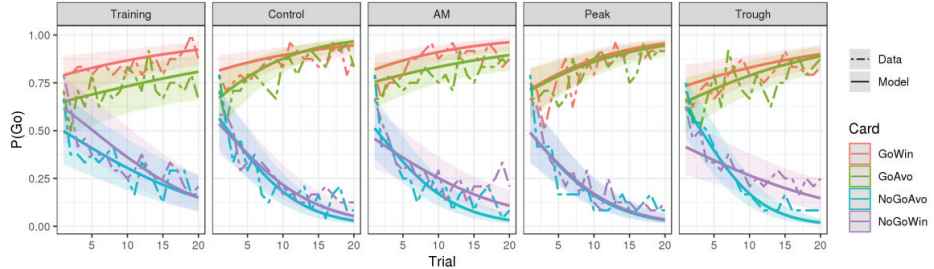
476 To assess learning performance across sessions, we fitted a series of hierarchical
477 Bayesian logistic regression models, treating accuracy as the dependent variable. All of
478 the models received a random intercept for each participant and for sessions nested
479 within participants. Furthermore, we included various combinations of the following
480 predictor variables: Card-type (four levels: Go-to-Win, NoGo-to-Avoid, Go-to-Avoid and
481 NoGo-to-Avoid), tACS session (five levels: Training, Control, AM, Peak and Trough),
482 Trial (Z-transformed trial number during each experimental session), Session order
483 (continuous predictor coding for the order in which the tACS sessions were conducted)
484 as well as their interactions. All of these 20 models were compared according to their

485 out-of-sample predictive performance using the LOOIC (Vehtari et al., 2017). Based on
486 this criterion, we calculated model weights using two different techniques: Based on
487 Akaike weights (Wagenmakers & Farrell, 2004) using the LOOIC instead of the AIC and
488 using Bayesian model averaging (BMA; Yao et al., 2018). Both of these techniques
489 resulted in posterior probabilities quantifying how likely it is that each of the models was
490 the best one.

491 After calculating these model selection criteria, we found converging evidence that
492 the model that encompassed all predictors, including all two-way and three-way
493 interactions between Card, tACS session and Trial, as well as a main effect of Session
494 order outperformed the other models (Akaike weight $p = 0.63$, next best model $p = 0.34$;
495 BMA weight $p = 0.47$, next best model $p = 0.23$).

496 We therefore based our conclusions on that winning model and investigated it in
497 detail. First, we checked that the model captured the trends in the data well. In Figure 3,
498 we plotted the raw data and overlaid predictions from the winning logistic regression
499 model (posterior predictive check). The model captured the trends in the data well and
500 the uncertainty (95% HDIs) around the model-predictions was sufficiently broad relative
501 to the fluctuations in the data. The Bayesian R^2 value for this model was $R^2 = 0.23$
502 HDI[0.22,0.24].

503



504

505 **Figure 3.** Posterior predictive checks for the final logistic regression model. The model
 506 predictions (solid lines) captured the main trends in the data (dashed lines) well. Colored
 507 ribbons are 95% HDIs. Abbreviations: AM – amplitude-modulated.

508

509 We focused on two separate aspects of the data: First, we investigated how the
 510 general accuracy level varied across cards and sessions. In the presence of the three-
 511 way interaction of Card \times tACS session \times Trial, we quantified and compared the
 512 accuracy level in the middle of each session. Second, we were interested in the learning
 513 rate with which accurate responding increased. In our model, this was manifested in the
 514 tACS session \times Trial, Card \times Trial and Card \times tACS session \times Trial interactions that
 515 allowed us to investigate the rate with which the correct way to respond to each of the
 516 cards was learned across the sessions.

517

518 3.3. Average accuracy

519 The accuracy levels as estimated by the model in the middle of each session are
 520 displayed in Figure 4. There was a significant amount of variation both between the
 521 cards and sessions. As expected, responses to the Go-to-Win card were generally most
 522 accurate ($b_{GoAvo} = -0.88[-1.24, -0.54]$, $b_{NoGoAvo} = -1.02[-1.39, -0.68]$, $b_{NoGoWin} =$

523 $-1.25[-1.63, -0.90]$) while the NoGo-to-Win card was most difficult with the other two
 524 cards being situated between.

525 Furthermore, we found a learning effect between the Training session (which was
 526 always the first session each participant was exposed to) and the other sessions (which
 527 were randomized): Performance was better in all tACS sessions and for all cards, the
 528 only exception being the Go-to-Win card in the Trough session ($P(Trough > Training \vee$
 529 $GoWin) = 0.23$). This learning-effect was not surprising given that this task is known to
 530 exhibit between-session learning effects (Csifcsák et al., 2020). However, after the initial
 531 effect of learning from the Training session to the second one, there was no clear further
 532 effect of Session order, $b_{order} = -0.08[-0.26, 0.10]$.

533

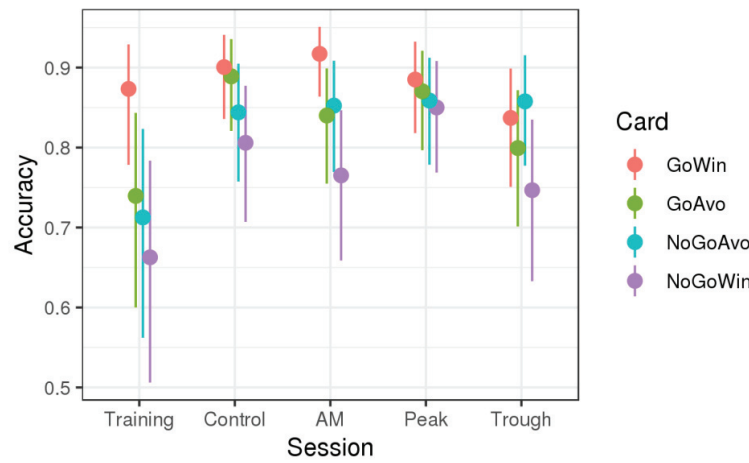


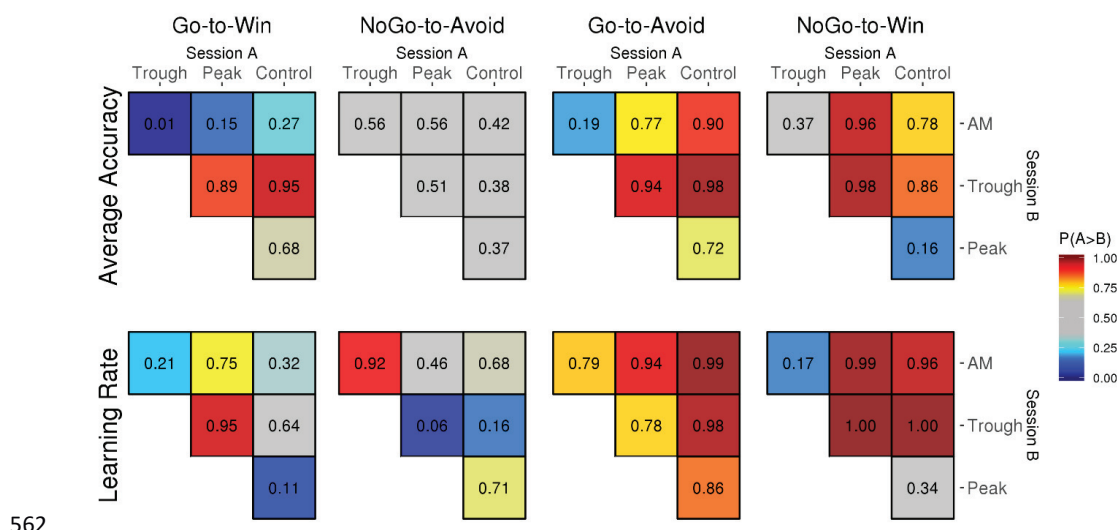
Figure 4. Estimated accuracy levels in the middle of the experimental session for each session and card. The colors represent the four card types, with the experimental sessions shown on the horizontal axis. Note that the participants received no tACS during the training session. Abbreviations: AM – amplitude-modulated tACS; control – control tACS.

534 We were interested in how general accuracy changed between the different tACS
535 sessions. A summary of the results is presented in Figure 5, upper row. Here, each entry
536 in the matrix documents the posterior probability that accuracy was increased from one
537 session (A) to the next (B). High values close to 1 (red) indicate that session A was
538 highly likely to show increased accuracy relative to session B while low values close to
539 zero indicate the opposite. Intermediate values (grey) mean that the results are
540 inconclusive for that particular comparison. For example, in the ‘Go to win’ card the
541 value of 0.95 in the middle row, right column suggests that it is highly probable that the
542 average accuracy was higher in the control tACS (session A) compared to the trough-
543 coupled tACS (session B).

544 We start by comparing the three active tACS sessions AM, Peak and Trough with
545 the Control session. The *p*-values given here represent the posterior probability that the
546 active session showed higher accuracy compared with the Control session (*i.e.*, the
547 probability that the difference *b* is positive) and are not to be confused with frequentist *p*-
548 values.

549 There was no clear difference between the AM and the Control session for
550 congruent cards (GoWin: $b = 0.21[-0.47,0.87]$, $p = 0.73$, NoGoAvo: $b = 0.06[-0.54,0.75]$, $p =$
551 0.58) with possibly a small performance decrease for conflicting cards (GoAvo: $b =$
552 $-0.43[-1.09,0.19]$, $p = 0.10$, $b = -0.25[-0.85,0.38]$, $p = 0.22$) though the HDIs for these
553 effects did not exclude zero. The Peak session did not result in a change in general
554 accuracy compared with Control for congruent (GoWin: $b = -0.15[-0.86,0.47]$, $p = 0.32$,
555 NoGoAvo: $b = 0.11[-0.52,0.76]$, $p = 0.63$) or conflicting cards (GoAvo:
556 $b = -0.19[-0.84,0.47]$, $p = 0.28$, NoGoWin: $b = 0.31[-0.32,0.95]$, $p = 0.84$). Finally, the

557 Trough session showed reduced accuracy particularly for the easiest Go-to-Win cards,
 558 $b = -0.56[-1.18,0.11], p = 0.05$ (but not for NoGo-to-Avoid, $b = 0.11[-0.55,0.74], p = 0.62$)
 559 and reduced accuracy for both conflicting cards (GoAvo: $b = -0.70[-1.33,-0.04], p = 0.02$,
 560 NoGo-to-Win: $b = -0.34[-0.95,0.29], p = 0.14$). Direct comparisons between the active
 561 stimulation sessions are also shown in Figure 5 (upper row).



562 **Figure 5.** Comparison of average accuracy (top row) and learning rate (bottom row)
 between tACS sessions for each of the four cards. Colors and numbers in the matrices
 indicate the probability that the session indicated by the column showed a stronger
 effect compared with the session indicated by the row of each matrix. Abbreviations: AM
 – amplitude-modulated.

563 3.4. Learning rate analysis

564 Next, we supplemented the analysis of the general accuracy with a parallel analysis
 565 regarding the learning rate, *i.e.*, Card and tACS session interactions with the Trial term
 566 in the model. In Figure 5 the lower row shows a summary of this analysis. AM and

567 Control sessions did not differ clearly for congruent cards (GoWin:
568 $b = 0.10[-0.30,0.52], p = 0.68$, NoGoAvo: $b = -0.09[-0.47,0.31], p = 0.32$), but learning
569 was decreased for conflicting cards (GoAvo: $b = -0.50[-0.88,-0.13], p = 0.01$,
570 NoGoWin: $b = -0.33[-0.69,0.02], p = 0.04$). For the Peak session, the results are
571 similar but less clear, with a possible small improvement for Go-to-Win cards ($b =$
572 $0.24[-0.14,0.58], p = 0.89$) but not NoGo-to-Avoid ($b = -0.11[-0.51,0.28], p = 0.29$) and
573 possibly a weak decrease for Go-to-Avoid cards ($b = -0.21[-0.61,0.18], p = 0.14$) but
574 not for the NoGo-to-Win cards ($b = 0.08[-0.30,0.44], p = 0.66$). For the Trough session,
575 we found no clear differences for congruent cards (GoWin: $b = -0.07[-0.41,0.31], p =$
576 0.36 , NoGoAvo: $b = 0.21[-0.22,0.59], p = 0.84$) but clear learning decreases for the
577 conflicting cards (GoAvo: $b = 0.36[-0.01,0.74], p = 0.02$, NoGoWin:
578 $b = 0.49[0.11,0.80], p = 0.00$).

579

580 **3.5. Perceptual adverse effects**

581 Most participants reported no cutaneous sensations during tACS, possibly due to the
582 application of the topical anesthetic cream. However, we also inspected the amount of
583 perceptual adverse effects, such as itching, tingling, and burning sensations, and
584 phosphenes that were reported following each tACS session. A careful inspection of the
585 subjectively reported perceptual adverse effects did not reveal any substantial
586 differences between the stimulation sessions.

587

588 **4. Discussion**

589 In this study, we investigated the behavioral effects of three active theta-gamma
590 CFC-tACS protocols in a cognitive control task. In the peak- and trough-coupled tACS

591 conditions, we coupled the short bursts of 80 Hz gamma tACS to the local maximum,
592 *i.e.*, peak, or minimum, *i.e.*, trough, of the 4 Hz theta tACS. In the amplitude-modulated
593 tACS condition, we modulated the amplitude of the 80 Hz gamma tACS by the phase of
594 the 4 Hz theta tACS. In the fourth condition, which served as a control, we continuously
595 coupled the 80 Hz gamma tACS to the 4 Hz theta tACS.

596 As we had hypothesized, we found that the trough-coupled tACS condition impaired
597 behavioral performance, in particular in the more challenging, conflicting trials. We
598 speculate that this protocol likely interfered with the phase-dependent theta-gamma
599 coupling between the cingulate (*e.g.*, ACC) and the prefrontal cortices (*e.g.*, DLPFC)
600 (Smith et al., 2015). In a previous study using a Stroop-like interference task, information
601 transfer analysis (Granger causality) showed that the feedback-related information
602 travels from the ACC to the DLPFC in the theta band (Smith et al., 2015). These findings
603 may suggest that the ACC presumably signals the need for cognitive control, whereas
604 the DLPFC processes this information and influences ongoing behavior by exerting
605 model-based behavioral control (Smith et al., 2015). Thus, the modulation of the
606 information flow from the cingulate to prefrontal cortex via theta-gamma CFC could have
607 impaired the model-based control in the trough-coupled tACS condition.

608 The observed behavioral effects in the present study may be due to the direct
609 stimulation of the frontal and cingulate cortices or to indirect network effects. It has been
610 shown in primates that there are monosynaptic connections between the frontal cortex,
611 including the ventromedial prefrontal and cingulate cortices, to the subthalamic nucleus
612 (Haynes & Haber, 2013). This pathway is called the hyperdirect pathway, which
613 supposedly exerts a strong top-down control on ongoing decisions: It influences whether
614 an action is performed or not (Frank, 2006). One of the proposed functional relevancies

615 of the hyperdirect pathway is to slow down the initial actions in cognitive control
616 situations, when it is crucial to quickly evaluate the expected outcome of different
617 behavioral alternatives (Frank, 2006). It is possible that the observed behavioral findings
618 in the present study are due to the notion that the trough-coupled tACS condition
619 indirectly interfered with the neural oscillation in the hyperdirect pathway.

620 At the same time, the trough-coupled tACS condition did not impair the average
621 accuracy but it may even have slightly improved the learning rate in one of the
622 congruent trials, *i.e.*, ‘NoGo to Avoid’. We note, however, that the statistical analysis
623 provided only inconclusive evidence for the improvement effect in the learning rate. We
624 therefore interpret this finding that the trough-coupled tACS condition had only negligible
625 effect if any on the ‘NoGo to Avoid’ decisions and that the main effect of the trough-
626 coupled tACS condition was inferential in nature.

627 Unexpectedly, the amplitude-modulated tACS condition slowed the learning rate for
628 the conflicting trials, which is reminiscent of the behavioral effects of the trough-coupled
629 tACS condition. However, its diminishing behavioral effect was less pronounced when
630 compared with the trough-coupled tACS condition. In the amplitude-modulated tACS
631 protocols, the slow, *i.e.*, the theta frequency, might have played an important role in
632 producing the cognitive effects of tACS (Minami & Amano, 2017). As increased power of
633 theta-range oscillations leads to better performance during cognitive conflict (Cavanagh
634 et al., 2013), we would expect behavioral improvement under this protocol. Previous
635 studies with single-frequency theta tACS showed beneficial behavioral effects in
636 cognitive control tasks, including reduced reaction time or facilitated behavioral accuracy
637 (Hsu et al., 2017; Lehr et al., 2019).

638 Contrary to our expectations, we found no clear and consistent behavioral effects for
639 the peak-coupled tACS protocol. In a previous study, Alekseichuk and colleagues (2016)
640 observed behavioral improvement in the sensitivity index of a spatial working memory
641 task during the peak-coupled tACS. Since the peak-coupled tACS protocol mimics the
642 phase-specificity of theta-gamma CFC when signaling the need for cognitive control
643 (Smith et al., 2015), we expected that it would increase the efficacy of the cingulate
644 cortex to signal the need for cognitive control and thereby increase the degree of model
645 based control implemented by the prefrontal cortex.

646 The lack of the behavioral effects could also have been due to the thorough
647 instructional procedure we used in the present study. The exhaustive instructional
648 procedure might have produced a ceiling effect, which could diminish the ability of the
649 stimulation to further improve the performance of our volunteers. We expect that the
650 peak-coupled tACS condition may improve the behavioral performance in groups of
651 participants who do not reach the ceiling effect, e.g., in elderly participants or in
652 individuals with mild cognitive impairment.

653 One of the limitations of the present study is that the computational modelling results
654 were inconclusive given that the model was unable to capture our participants' behavior.
655 Therefore, we can neither confirm nor falsify our third hypothesis concerning the
656 underlying cognitive processes (*i.e.*, Pavlovian bias parameter). We speculate that the
657 lack of fit of our computational models could be, at least partially, due to the instructional
658 procedure we used in this study. Specifically, our participants received very thorough
659 instructions about the task including reading the written instruction, listening to the verbal
660 explanation of the experimenter, performing the short practice, filling out the
661 questionnaire about the task, and performing the training session. By this procedure, we

662 initially intended to minimize the probability that the participants would misunderstand
663 the task and make their decisions in a random fashion. However, the exhaustive
664 instructional procedure likely affected the strategy of the participants, who performed
665 very well on the task. In fact, even though our task was more difficult than that used in
666 previous studies (e.g., in Cavanagh et al., 2013), the overall accuracy level in the tACS
667 sessions was higher in our study indicating that the participants were potentially able to
668 exploit the task structure to improve their reward rate.

669 Evidence exists that the task instruction can indirectly influence how humans perform
670 an instrumental learning task. This phenomenon is known in the literature as the
671 behavioral rule-governing effect (Doll et al., 2009). It is possible that after the
672 instructional phase at least some participants were able to infer the correct structure of
673 the task, even before the direct experience. This may have facilitated the learning
674 process through the mechanism of confirmation bias (Doll et al., 2009); participants
675 learned quickly to amplify those outcomes that were consistent with their internal model
676 of the task and discarded the incompatible ones. Given the relatively difficult reward
677 contingency probabilities (0.65 vs 0.35), we expected much more exploration in the
678 initial phase of the task (e.g., Csifcsák et al., 2020).

679 This argument is further supported by the results of the qualitative analysis we
680 performed about the explicit knowledge of the card types. We found that all participants
681 were able to correctly identify both the valence and the action value of the cards in the
682 overwhelming majority of the cases (approx. 91%). Occasionally, the participants made
683 mistakes when identifying the correct action to the valence (approx. 8%). Other error
684 types were very rare. We interpret these findings as a further indirect support that the
685 participants had explicit, rule-based knowledge about the structure of the task.

686 By using a less thorough instructional procedure, future studies may use
687 computational modeling (e.g., in Csifcsák et al., 2020) to explore the hidden parameters
688 that may be influenced by the CFC-tACS protocol. Because these models assume that
689 participants do gradually learn the expected value of the stimulus (Cavanagh et al.,
690 2013; Csifcsák et al., 2020), we were not able to utilize them fruitfully in the present
691 study.

692 Another possible limitation of the present study is the lack of a sham tACS protocol.
693 Because real tACS can induce both cutaneous and visual perceptual adverse effects
694 during the entire stimulation period, we preferred using a control tACS protocol, instead
695 of a sham tACS protocol (Turi et al., 2013). The conventionally used fade-in, short-
696 stimulation, fade-out sham protocols, may not be able to maintain effective blinding for
697 the real intervention due to their shortness, as has been shown for transcranial direct
698 current stimulation (Greinacher et al., 2019; Turi et al., 2019).

699 According to an alternative explanation, the control condition might have improved
700 the behavioral performance to a similar extent to the peak-coupled tACS condition but
701 slightly stronger than in the amplitude-modulated tACS condition. Given that the theta
702 and gamma tACS were continuously superimposed in the control condition, this protocol
703 had equal chance to improve or impair the behavioral performance. Therefore, this
704 alternative explanation does not explain why the control stimulation would have
705 improved, rather than impaired the performance. Second, a previous study applying a
706 closely matched control protocol found no cognitive effect on a cued-recall task, even
707 when comparing the cognitive performance before and after the intervention (Amador de
708 Lara et al., 2017). Therefore, we find this alternative explanation to be less likely.

709 Taken together, CFC-tACS protocols can extend single-frequency tACS protocols by
710 enabling the testing of CFC phenomena intrinsic to endogenous network oscillations
711 (Alekseichuk et al., 2016; Bächinger et al., 2017; Minami & Amano, 2017). In this study,
712 we showed that trough-coupled tACS, *i.e.*, when gamma tACS was coupled over the
713 trough of theta tACS, and amplitude-modulated tACS decreased the behavioral
714 performance and the use of cognitive control in healthy participants. These findings
715 suggest that the phase of coupling between theta and gamma frequencies may play an
716 important role in cognitive control.

717

718 **Extended Data 1** - Extended data 1 contains all materials, pseudonymized raw data
719 and analysis scripts used in this study that are freely available at our repository.

720

721

722 **5. References**

- 723 Ahn, W.-Y., Haines, N., & Zhang, L. (2017). Revealing Neurocomputational Mechanisms
724 of Reinforcement Learning and Decision-Making With the hBayesDM Package.
725 *Computational Psychiatry*, 1(Figure 1), 24–57.
726 https://doi.org/10.1162/cpsy_a_00002
- 727 Alekseichuk, I., Turi, Z., Amador de Lara, G., Antal, A., & Paulus, W. (2016). Spatial
728 Working Memory in Humans Depends on Theta and High Gamma Synchronization
729 in the Prefrontal Cortex. *Current Biology*, 26(12), 1513–1521.
730 <https://doi.org/10.1016/j.cub.2016.04.035>
- 731 Amador de Lara, G., Alekseichuk, I., Turi, Z., Lehr, A., Antal, A., & Paulus, W. (2017).
732 Perturbation of theta-gamma coupling at the temporal lobe hinders verbal
733 declarative memory. *Brain Stimulation*, 1–9.
734 <https://doi.org/10.1016/j.brs.2017.12.007>
- 735 Bächinger, M., Zerbi, V., Moisa, M., Polania, R., Liu, Q., Martini, D., Ruff, C., &
736 Wenderoth, N. (2017). Concurrent tACS-fMRI Reveals Causal Influence of Power
737 Synchronized Neural Activity on Resting State fMRI Connectivity. *The Journal of
738 Neuroscience*, 37(18), 4766–4777. <https://doi.org/10.1523/JNEUROSCI.1756-16.2017>
- 740 Bürkner, P. C. (2018). Advanced Bayesian multilevel modeling with the R package brms.
741 *The R Journal*, 10(1), 395–411. <https://doi.org/10.32614/rj-2018-017>

- 742 Canolty, R. T., & Knight, R. T. (2010). The functional role of cross-frequency coupling.
743 *Trends in Cognitive Sciences*, 14(11), 506–515.
744 <https://doi.org/10.1016/j.tics.2010.09.001>
- 745 Carpenter, B., Gelman, A., Hoffman, M., Lee, D., Goodrich, B., Betancourt, M.,
746 Brubaker, M. A., Li, P., & Riddell, A. (2017). Stan : A Probabilistic Programming
747 Language. *Journal of Statistical Software*, 76(1), 2–32.
- 748 Cavanagh, J. F., Eisenberg, I., Guitart-Masip, M., Huys, Q., & Frank, M. J. (2013).
749 Frontal Theta Overrides Pavlovian Learning Biases. *Journal of Neuroscience*,
750 33(19), 8541–8548. <https://doi.org/10.1523/JNEUROSCI.5754-12.2013>
- 751 Cavanagh, J. F., & Frank, M. J. (2014). Frontal theta as a mechanism for cognitive
752 control. *Trends in Cognitive Sciences*, 18(8), 414–421.
753 <https://doi.org/10.1016/j.tics.2014.04.012>
- 754 Cohen, M. X. (2014). A neural microcircuit for cognitive conflict detection and signaling.
755 *Trends in Neurosciences*, 37(9), 480–490. <https://doi.org/10.1016/j.tins.2014.06.004>
- 756 Csifcsák, G., Melsæter, E., & Mittner, M. (2020). Intermittent Absence of Control during
757 Reinforcement Learning Interferes with Pavlovian Bias in Action Selection. *Journal
758 of Cognitive Neuroscience*, 32(4), 646–663.
- 759 Doll, B. B., Jacobs, W. J., Sanfey, A. G., & Frank, M. J. (2009). Instructional control of
760 reinforcement learning : A behavioral and neurocomputational investigation. *Brain
761 Research*, 1299, 74–94. <https://doi.org/10.1016/j.brainres.2009.07.007>
- 762 Frank, M. J. (2006). Hold your horses: A dynamic computational role for the subthalamic

- 763 nucleus in decision making. *Neural Networks*, 19(8), 1120–1136.
- 764 <https://doi.org/10.1016/j.neunet.2006.03.006>
- 765 Gelman, A., & Rubin, D. B. (1992). Interference from iterative simulation using multiple
766 sequences. *Statistical Science*, 7(4), 457–511.
767 <https://doi.org/10.1214/ss/1177013437>
- 768 Greinacher, R., Buhôt, L., Möller, L., & Learmonth, G. (2019). The time course of
769 ineffective sham-blinding during low-intensity (1 mA) transcranial direct current
770 stimulation. *European Journal of Neuroscience*, 50(8), 3380–3388.
771 <https://doi.org/10.1111/ejn.14497>
- 772 Guitart-Masip, M., Chowdhury, R., Sharot, T., Dayan, P., Duzel, E., & Dolan, R. J.
773 (2012). Action controls dopaminergic enhancement of reward representations.
774 *Proceedings of the National Academy of Sciences*, 109(19), 7511–7516.
775 <https://doi.org/10.1073/pnas.1202229109>
- 776 Guitart-Masip, M., Duzel, E., Dolan, R., & Dayan, P. (2014). Action versus valence in
777 decision making. *Trends in Cognitive Sciences*, 18(4), 194–202.
778 <https://doi.org/10.1016/j.tics.2014.01.003>
- 779 Haynes, W. I. A., & Haber, S. N. (2013). The organization of prefrontal-subthalamic
780 inputs in primates provides an anatomical substrate for both functional specificity
781 and integration: Implications for basal ganglia models and deep brain stimulation.
782 *Journal of Neuroscience*, 33(11), 4804–4814.
783 <https://doi.org/10.1523/JNEUROSCI.4674-12.2013>

- 784 Helfrich, R. F., & Knight, R. T. (2019). Cognitive neurophysiology of the prefrontal cortex.
- 785 In *Handbook of Clinical Neurology* (1st ed., Vol. 163). Elsevier B.V.
- 786 <https://doi.org/10.1016/B978-0-12-804281-6.00003-3>
- 787 Hsu, W. Y., Zanto, T. P., Schouwenburg, M. R. V., & Gazzaley, A. (2017). Enhancement
- 788 of multitasking performance and neural oscillations by transcranial alternating
- 789 current stimulation. *PlosOne*, 1–17.
- 790 Kruschke, J. (2014). *Doing Bayesian data analysis: A tutorial with R, JAGS, and Stan*.
- 791 Academic Press.
- 792 Lehr, A., Henneberg, N., Nigam, T., Paulus, W., & Antal, A. (2019). Modulation of
- 793 Conflict Processing by Theta-Range tACS over the Dorsolateral Prefrontal Cortex.
- 794 *Neural Plasticity*.
- 795 Minami, S., & Amano, K. (2017). Illusory Jitter Perceived at the Frequency of Alpha
- 796 Report Illusory Jitter Perceived at the Frequency of Alpha Oscillations. *Current*
- 797 *Biology*, 27(15), 2344-2351.e4. <https://doi.org/10.1016/j.cub.2017.06.033>
- 798 Negahbani, E., Kasten, H. F., Herrmann, C. S., & Fröhlich, F. (2018). Targeting Alpha-
- 799 band Oscillations in a Cortical Model with Amplitude-Modulated High-Frequency
- 800 Transcranial Electric Stimulation. *Neuroimage*, 173, 3–12.
- 801 <https://doi.org/10.1016/j.physbeh.2017.03.040>
- 802 Peirce, J. W. (2007). PsychoPy-Psychophysics software in Python. *Journal of*
- 803 *Neuroscience Methods*, 162(1–2), 8–13.
- 804 <https://doi.org/10.1016/j.jneumeth.2006.11.017>

- 805 Peirce, J. W. (2009). Generating stimuli for neuroscience using PsychoPy. *Frontiers in*
806 *Neuroinformatics*, 2(10), 1–8. <https://doi.org/10.3389/neuro.11.010.2008>
- 807 Peterchev, A. V., Wagner, T. A., Miranda, P. C., Nitsche, M. A., Paulus, W., Lisanby, S.
808 H., Pascual-leone, A., & Carolina, N. (2012). Fundamentals of transcranial electric
809 and magnetic stimulation dose: Definition , selection , and reporting practices. *Brain*
810 *Stimulation*, 5(4), 435–453. <https://doi.org/10.1016/j.brs.2011.10.001>
- 811 Shenhav, A., Musslick, S., Lieder, F., Kool, W., Griffiths, T. L., Cohen, J. D., & Botvinick,
812 M. M. (2017). Toward a Rational and Mechanistic Account of Mental Effort. *Annual*
813 *Review of Neuroscience*, 40, 99–124.
- 814 Smith, X. E. H., Banks, X. G. P., Mikell, C. B., Cash, X. S. S., Patel, S. R., Eskandar, E.
815 N., & Sheth, S. A. (2015). Frequency-Dependent Representation of Reinforcement-
816 Related Information in the Human Medial and Lateral Prefrontal Cortex. *The Journal*
817 *of Neuroscience*, 35(48), 15827–15836. <https://doi.org/10.1523/JNEUROSCI.1864-15.2015>
- 819 Team, R. C. (2018). *R: A language and environment for statistical computing*. R
820 Foundation for Statistical Computing. <https://www.r-project.org/>
- 821 Team, Rs. (2016). *RStudio: Integrated Development for R*. RStudio, Inc., Boston, MA.
- 822 Team, S. D. (2018). *RStan: The R Interface to Stan*. <http://mc-stan.org/>
- 823 Thielscher, A., Antunes, A., & Saturnino, G. B. (2015). Field modeling for transcranial
824 magnetic stimulation: A useful tool to understand the physiological effects of TMS?
825 *Proceedings of the Annual International Conference of the IEEE Engineering in*

- 826 *Medicine and Biology Society, EMBS*, 222–225.
- 827 <https://doi.org/10.1109/EMBC.2015.7318340>
- 828 Turi, Z., Ambrus, G. G., Janacsek, K., Emmert, K., Hahn, L., Paulus, W., & Antal, A.
- 829 (2013). Both the cutaneous sensation and phosphene perception are modulated in
- 830 a frequency-specific manner during transcranial alternating current stimulation.
- 831 *Restorative Neurology and Neuroscience*, 31(3), 275–285.
- 832 <https://doi.org/10.3233/RNN-120297>
- 833 Turi, Z., Opitz, A., Groot, J., Thielscher, A., & Hawkins, G. E. (2019). *Blinding is*
- 834 *compromised for transcranial direct current stimulation at 1 mA for 20 min in young*
- 835 *healthy adults. February*, 1–8. <https://doi.org/10.1111/ejn.14403>
- 836 Vehtari, A., Gelman, A., & Gabry, J. (2017). Practical Bayesian model evaluation using
- 837 leave-one-out cross-validation and WAIC. *Statistics and Computing*, 27(5), 1413–
- 838 1432. <https://doi.org/10.1007/s11222-016-9696-4>
- 839 Wagenmakers, E. J., & Farrell, S. (2004). AIC model selection using Akaike weights.
- 840 *Psychonomic Bulletin and Review*, 11(1), 192–196.
- 841 <https://doi.org/10.3758/BF03206482>
- 842 Yao, Y., Vehtari, A., Simpson, D., & Gelman, A. (2018). Using Stacking to Average
- 843 Bayesian Predictive Distributions (with Discussion). *Bayesian Analysis*, 13(3), 917–
- 844 1007. <https://doi.org/10.1214/17-ba1091>

845 **6. Authors contribution**

846 ZT: conceptualization, study design, project administration, methodology, software
847 (behavioral paradigm), supervised data collection, supervised medical student, prepared
848 illustrations, data visualization, interpreted data, data curation, wrote original draft and
849 revised manuscript.

850 MM: formal statistical analysis, data visualization, computational modelling of behavioral
851 data, interpreted data, data curation, wrote original draft and revised manuscript.

852 AL: contributed to formal analysis, contributed to preparing illustrations, data
853 visualization, interpreted data and wrote original draft and revised manuscript.

854 HB: data collection (as part of her medical dissertation at the University Medical Center
855 Göttingen, Germany, supervised by author AA), transcribed data, contributed to writing
856 original draft and revised manuscript.

857 AA: project administration, supervised medical student, contributed to writing original
858 draft and revised manuscript.

859 WP: study design, resources and funding acquisition, contributed to writing original draft
860 and revised manuscript.

861

862 **7. Acknowledgements**

863 The authors wish to thank Dr. med. Anja Manig, Dr. med. Sebastian Schade, Dr. med.
864 Dirk Czesnik and Dr. med. Claire Halsband for the neurological examinations. We thank
865 Prof. Thomas Crozier for his comments on the manuscript.

866 **8. Conflict of interest**

867 Authors report no conflict of interest.

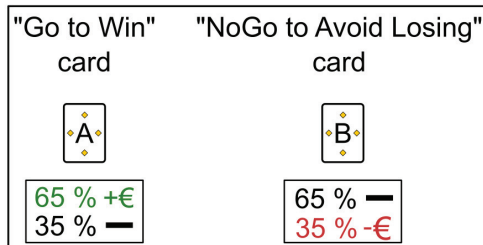
868

869 **9. Funding sources**

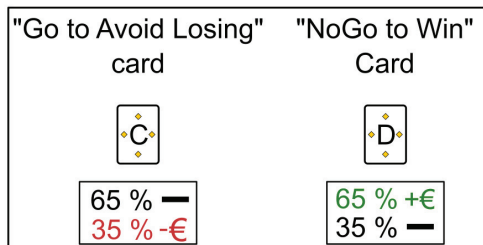
870 This research was financially supported by DFG PA 419/15-1 awarded to WP. AL was
871 supported by the IMPRS Neurosciences. AA was supported by the State of Lower
872 Saxony, Germany (76251-12-7/19 (ZN 3456))

A Learning phase

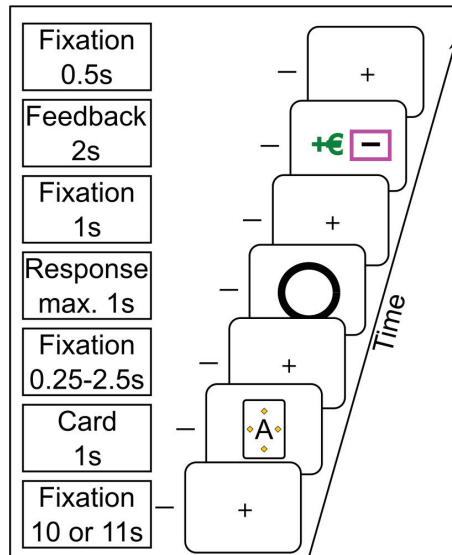
Pavlovian congruent



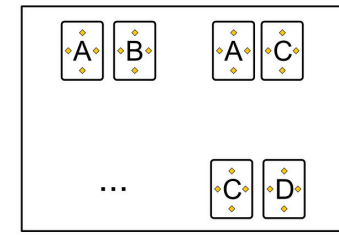
Pavlovian conflict



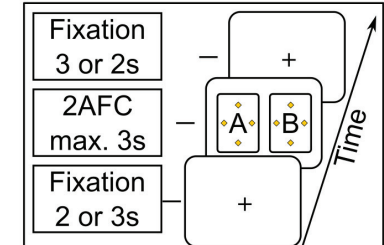
Trial flow

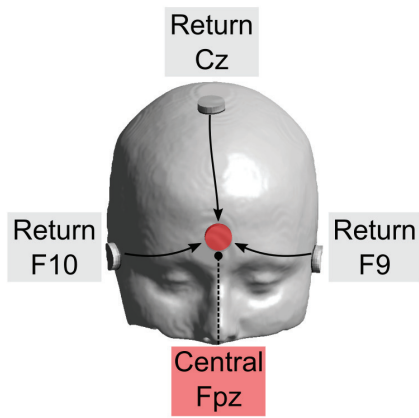
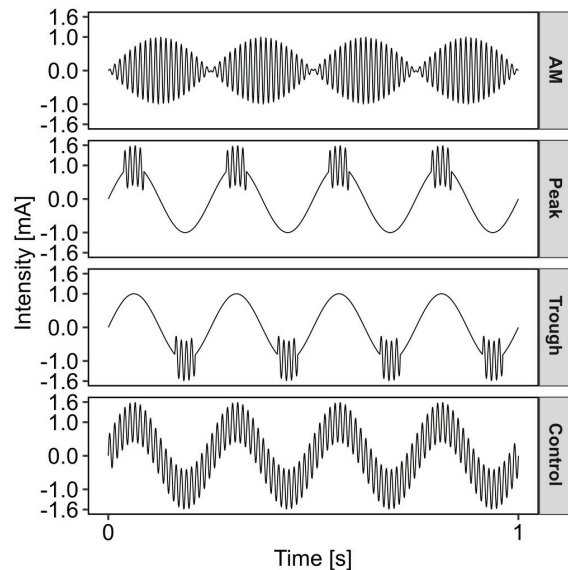
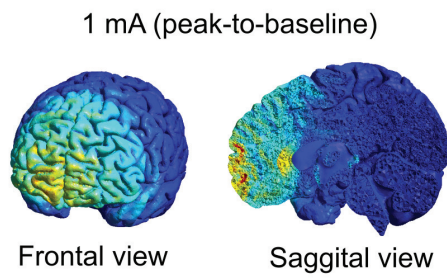
**B Transfer phase**

All card combinations



Trial flow



A Electrode montage**B Waveforms of CFC-tACS protocols****C Estimated induced electric field magnitudes**

Electric field [mV/mm]
0 0.3

